Large-scale shell-model calculation with core excitations for neutron-rich nuclei beyond ^{132}Sn

Hua Jin (金华),[1,2] Munetake Hasegawa (长谷川宗武),[1,3] Shigeru Tazaki (田崎茂),[4] Kazunari Kaneko (金子和也),[5] and Yang Sun (孙扬)[1,3,6,*]

[1]*Department of Physics, Shanghai Jiao Tong University, Shanghai 200240, People's Republic of China*
[2]*Department of Mathematics and Physics, Shanghai Dianji University, Shanghai 200240, People's Republic of China*
[3]*Institute of Modern Physics, Chinese Academy of Sciences, Lanzhou 730000, People's Republic of China*
[4]*Department of Applied Physics, Fukuoka University, Fukuoka 814-0180, Japan*
[5]*Department of Physics, Kyushu Sangyo University, Fukuoka 813-8503, Japan*
[6]*Department of Physics and Astronomy, University of Tennessee, Knoxville, Tennessee 37996, USA*

(Received 18 August 2011; published 24 October 2011)

The structure of neutron-rich nuclei with a few nucleons beyond ^{132}Sn is investigated by means of large-scale shell-model calculations. For a considerably large model space, including neutron core excitations, a new effective interaction is determined by employing the extended pairing-plus-quadrupole model with monopole corrections. The model provides a systematical description for energy levels of $A = 133$–135 nuclei up to high spins and reproduces available data of electromagnetic transitions. The structure of these nuclei is analyzed in detail, with emphasis of effects associated with core excitations. The results show evidence of hexadecupole correlation in addition to octupole correlation in this mass region. The suggested feature of magnetic rotation in ^{135}Te occurs in the present shell-model calculation.

DOI: 10.1103/PhysRevC.84.044324 PACS number(s): 21.10.−k, 21.60.Cs, 27.60.+j

I. INTRODUCTION

Near a doubly closed-shell nucleus, low-lying spectroscopy of valence nuclei with one particle in empty shells or one hole in completely filled shells gives direct information on the single-particle structure, while that of nuclei with two particles or two holes with respect to the double-shell closure can provide useful information on correlations between different kinds of pairs of valence nucleons. Recently, the magic nature of ^{132}Sn has been reconfirmed through a direct observation of single-particle states in ^{133}Sn [1]. The simplicity of ^{132}Sn, and the single-neutron excitations in ^{133}Sn, as well as those near this doubly closed-shell nucleus, provide a new touchstone needed for extrapolations to nuclei farther from stability [1].

Nuclei with a few valence particles outside a doubly closed shell have played an essential role in testing nuclear shell models. Detailed spectroscopic data are needed for this purpose, especially those from exotic mass regions. In the past decade, experiments have been accumulating data for nuclei beyond ^{132}Sn (see, for example, Refs. [2–11]). This enables us to reveal various interesting phenomena such as the properties of core excitation [7–10] to learn the magicity properties at $N = 82$. Among those excited high-spin states, spin isomers may appear [9–11], which usually carry valuable structure information. There have been motivated theoretical studies such as how the structure changes when nucleon number increases toward the drip line [12,13]. Moreover, the investigation on structure is crucially related to elucidating questions on nucleosynthesis [14] in this region. Shell model β-decay half-lives and neutron emission probabilities for the $N = 82$ waiting-point nuclei in the r process have been found to differ significantly from those calculated by the traditional methods, thus calling for extensive applications of quantitative shell models in nuclear astrophysics [15].

The relatively simple structure of near doubly closed-shell nuclei is recognized in their observed spectra which are usually understood as consisting of two types of excitations: excitations of valence single particles and excited states formed by couplings of the valence nucleons to core excitations. There have been successful calculations for the nuclei beyond ^{132}Sn. These calculations may be divided into two classes, treating, respectively, the two types of excitations. The low-energy states were studied microscopically by using the shell-model method, with the effective interaction derived from the CD-Bonn NN potential [13,16–19]. The interaction has been proven remarkably successful for the low-energy states of this mass region, which was demonstrated, for example, in the systematical study of the $N = 82$ isotones [17]. On the other hand, the high-energy (and often high-spin) states of core excitations were simply interpreted with empirical nucleon-nucleon interactions [8–10,20]. These two classes of calculations work for their own applicable states and have contributed greatly to the structure analysis in the mass region. Nevertheless, to study the interplay between them and understand the structure problem as a whole, it is desired to have a unified treatment for the two types of excited states in a manageable shell-model calculation. The challenging question is to find out suitable effective shell-model interactions that work for the description of both types of excitation.

If high-energy states are constructed by neutron core excitations across the $N = 82$ closed shell, descriptions of these states require several neutron orbits to be considered in the upper and lower part of the $N = 82$ shell gap. To determine practically two-body interaction matrix elements for this kind of study, the extended paring-plus-quadrupole model with monopole corrections (EPQQM) [21] may be a hopeful method. The EPQQM model has demonstrated its

*sunyang@sjtu.edu.cn

applicability in nuclei where protons and neutrons occupy the same orbits. It has been shown that the obtained results for the fp-shell nuclei ($A = 42$–51) [22] and $f_{5/2}pg_{9/2}$-shell nuclei ($A = 62$–68) [23] are very similar to those obtained with the realistic effective interactions. The EPQQM model has also been applied to nuclei in which protons and neutrons occupy different orbits. For example, it explains well the complicated energy levels in ^{94,95}Mo [24] and the neighboring nuclei, including the isomeric state $21/2^+$ in ^{93}Mo [25]. A study for neutron-rich sd-shell nuclei by the EPQQM model has recently been presented [26].

The use of separable forces in the nuclear Hamiltonian has advantages in its simplicity and flexibility. We note, in particular, that the EPQQM model requires only a few parameters to determine the interactions. The application of the pairing and quadrupole interactions has a long history in the nuclear structure study [27–29], which considers the two most important excitation modes in nuclei. A successful example is given by the projected shell model [30] which, by employing pairing-plus-quadrupole type of Hamiltonian, has demonstrated its ability to describe a large body of spectroscopic data in heavy, deformed nuclei. The success has its solid theoretical foundation. In fact, it has been pointed out by Dofour and Zuker [31] that the interactions with explicit multipole-multipole and pairing terms simulate the essence of the most important correlations in nuclei, so even realistic forces have to contain at least these basic components implicitly in order to work successfully in structure calculations. However, it is not clear, prior to the study, whether these forces are good enough for the exotic neutron-rich ^{132}Sn mass region. For another important aspect, a successful description of the spectroscopic data needs additional monopole corrections [32] in the Hamiltonian that guarantee the correct average energies of configurations. The monopole driven effect may be important for the evolution of the $N = 82$ shell gap near ^{132}Sn [33]. Otsuka *et al.* have pointed out [34] that, generally, due to tensor interactions, the nuclear mean field undergoes variations with neutron excess, which leads to monopole migration. More recently, a monopole-based universal interaction that consists of the central force in addition to the tensor force has also been introduced [35]. However, the monopole corrections that are needed for quantitative descriptions of spectroscopy in this mass region have not been explored.

The present article is devoted to finding a workable interaction for shell-model calculations for nuclei with a few valence particles outside ^{132}Sn. It is hoped that with this interaction, the entire excitation pattern from the low- to high-energy region can be studied as a whole. We do so by constructing the Hamiltonian within the framework of the EPQQM model and by applying a considerably large model space, including neutron core excitations. We show that the model provides a basic understanding for the energy levels of $A = 133$–135 nuclei up to high spins and reproduces available data of electromagnetic transitions. In the analysis of structure of these nuclei, we emphasize the discussions on the effects associated with core excitations. We also show that the early suggested feature of magnetic rotation in ^{135}Te occurs in the present shell-model calculation. Meanwhile, we point out those results showing clear discrepancies with data, which may indicate deficiencies in the present interaction and the chosen model space.

This paper is organized as follows. In Sec. II, we outline the EPQQM model and present the model space, the single-particle energies, and the parameters of the EPQQM interaction for the nuclei under consideration. In Sec. III, we discuss the calculated results of $A = 133$–135 nuclei in detail by showing comparisons with available experimental data and with other previous theoretical calculations. Finally, conclusions are drawn in Sec. IV.

II. OUTLINE OF THE THEORY

A. The EPQQM model

For the present shell-model calculation, separable forces are employed as effective interactions. In the previous study with the EPQQM model [21–23], the $J = 0$ and $J = 2$ pairing (P_0 and P_2) terms, the quadrupole-quadrupole (QQ) term, the octupole-octupole (OO) term, and the monopole corrections ($H_{\rm mc}$) were included in the Hamiltonian. The OO force may be important for nuclei under consideration [36] where, similar to the well-known octupole vibrations in the ^{208}Pb region, the 3^- particle-hole excitation across the $N = 82$ closed shell was observed [37]. In addition, we include the hexadecupole-hexadecupole (HH) force in the present calculations.

We write the Hamiltonian as follows:

$$\begin{aligned} H &= H_{\rm sp} + H_{P_0} + H_{P_2} + H_{QQ} + H_{OO} + H_{HH} + H_{\rm mc} \\ &= \sum_{\alpha} \varepsilon_a c^\dagger_\alpha c_\alpha - \frac{1}{2}\sum_{J=0,2} g_J \sum_{M\kappa} P^\dagger_{JM1\kappa} P_{JM1\kappa} \\ &\quad -\frac{1}{2}\frac{\chi_2}{b^4}\sum_M :Q^\dagger_{2M} Q_{2M}: -\frac{1}{2}\frac{\chi_3}{b^6}\sum_M :O^\dagger_{3M} O_{3M}: \\ &\quad -\frac{1}{2}\frac{\chi_4}{b^8}\sum_M :H^\dagger_{4M} H_{4M}: \\ &\quad +\sum_{a\leqslant b}\sum_T k^T_{\rm mc}(ab)\sum_{JM\kappa} A^\dagger_{JMT\kappa}(ab) A_{JMT\kappa}(ab), \end{aligned} \tag{1}$$

where $H_{\rm sp}$ is the single-particle Hamiltonian. $P^\dagger_{JM1\kappa}$ is the pair creation operator with angular momentum J and isospin $T = 1$. $Q^\dagger_{2M}$, $O^\dagger_{3M}$, and $H^\dagger_{4M}$ are the creation operators of the quadrupole, octupole, and hexadecupole terms, respectively, and the symbol :: denotes the normal order product of four nucleon operators. The corresponding force strengths χ_2, χ_3, and χ_4 are defined to have the dimension of energy by excluding the harmonic-oscillator range parameter b. Finally, $A^\dagger_{JMT\kappa}$ in Eq. (1) is a general pair operator, defined in the spin-isospin space as:

$$\begin{aligned} A^\dagger_{JMT\kappa}(ab) &= \sum_{m_\alpha m_\beta} \langle j_a m_\alpha j_b m_\beta | JM\rangle \\ &\quad \times \sum_{\rho\rho'} \left\langle \frac{1}{2}\rho\frac{1}{2}\rho' \middle| T\kappa \right\rangle \frac{c^\dagger_{\alpha\rho} c^\dagger_{\beta\rho'}}{\sqrt{1+\delta_{ab}}}. \end{aligned} \tag{2}$$

For the neutron-rich nuclei studied in the present paper, protons and neutrons essentially occupy different orbits. We, therefore,

use different force strengths g_0, g_2, χ_2, χ_3, and χ_4 for proton-proton (pp), neutron-neutron (nn), and proton-neutron (pn) interactions. It turns out that the total number of parameters in our model is 3×5, plus the single-particle energies ε_a of protons and neutrons and the strength parameters $k^T_{\rm mc}(ab)$ for the pp, nn, and pn monopole corrections.

The strengths of the multipole pairing and multipole-multipole forces are mass dependent in the usual treatment. The previous EPQQM model used mass-dependent force strengths for g_0, g_2, χ_2, and χ_3 [22,23]. However, there is a freedom for us to choose whether we treat the strengths as mass dependent. Considering that nuclei in the ^{132}Sn region have relatively large masses A, changes of the force strengths depending on A may be neglected if calculations do not go very far away from ^{132}Sn. When we adopt this approximation, our discussion for calculated results becomes simpler for the following reason. The observed energy levels of ^{133}Sn, ^{133}Sb, ^{131}Sn, and ^{131}In provide information about the particle and hole energies of proton and neutron. These particle and hole energies, however, may differ from "single-particle energies" in the shell-model basis because the observed particle and hole energies are usually the "dressed" ones by particle-hole interactions. Therefore, if the employed interactions have a mass dependence, theoretical particle and hole energies become, in principle, also mass dependent, and the shell-model single-particle energies must be changed for respective nuclei. This is somewhat troublesome for a theoretical discussion, especially for such an exotic mass region where our knowledge on structure is still rather limited. Therefore, we choose a conservative approach in the present paper: We use fixed force strengths of the EPQQM interaction for simplicity and, correspondingly, a fixed set of single-particle energies and interaction matrix elements common to all nuclei under consideration.

B. The model space

The low energy levels of ^{133}Sb (^{133}Sn) are considered to give single-particle energies for protons (neutrons) based on the doubly closed-shell nucleus ^{132}Sn with $Z = 50$ and $N = 82$. As the main emphasis of the present paper is core excitations, we choose the following single-particle orbits in the model space which considers neutron hole states as much as possible before the space becomes too large to handle: five proton orbits ($0g_{7/2}$, $1d_{5/2}$, $2s_{1/2}$, $1d_{3/2}$, and $0h_{11/2}$), five upper neutron orbits ($1f_{7/2}$, $2p_{3/2}$, $0h_{9/2}$, $2p_{1/2}$, and $1f_{5/2}$), and two lower neutron orbits ($0h_{11/2}$ and $1d_{3/2}$). Here we neglect the quite low proton orbit $0g_{9/2}$, the lower neutron orbits $0g_{7/2}$, $1d_{5/2}$, $2s_{1/2}$, and other orbits which are rather separated from the orbits shown above. Adopting this model space is so to consider valence nucleons in the orbits outside the frozen ^{116}Sn core with $Z = 50$ and $N = 66$.

We give below a concrete example about configurations. In ^{133}Sb, electromagnetic transitions have been observed from the states created by one-neutron particle-hole excitations with positive parity to those with negative parity [9,10]. This suggests contributions of two neutrons in the excitation. Therefore, we take the following configurations as the basis states for ^{133}Sb:

$$c^\dagger_\alpha(\pi)|^{132}\mathrm{Sn}\rangle, \quad c^\dagger_\alpha(\pi)c^\dagger_\beta(\nu)c_\gamma(\nu)|^{132}\mathrm{Sn}\rangle,$$
$$c^\dagger_\alpha(\pi)c^\dagger_\beta(\nu)c^\dagger_{\beta'}(\nu)c_\gamma(\nu)c_{\gamma'}(\nu)|^{132}\mathrm{Sn}\rangle, \tag{3}$$

with

$$|^{132}\mathrm{Sn}\rangle = \nu(0h_{11/2}, 1d_{3/2})^{16}|^{116}\mathrm{Sn\ core}\rangle.$$

In the above expression, $c^\dagger_\alpha(\pi)$ creates one proton in the orbits above $0g_{9/2}$, $c^\dagger_\beta(\nu)$ creates one neutron in the upper orbits ($1f_{7/2}$, $2p_{3/2}$, $0h_{9/2}$, $2p_{1/2}$, $1f_{5/2}$), and $c_\gamma(\nu)$ annihilates one neutron in the lower orbits ($0h_{11/2}$, $1d_{3/2}$). We neglect higher-order particle-hole excitations of more than one neutron from the same lower orbit for all nuclei considered in this paper.

Calculations are carried out with NUSHELLX, coded by W. Rae [38]. This code can treat systems with different proton and neutron orbitals and with different pp, nn, and pn interactions. The ordinary shell-model code does not perform calculations in the particle-hole representation. For example, a proton particle state $c^\dagger_\alpha(\pi)|^{132}\mathrm{Sn\ core}\rangle$ is calculated in the configuration of 1 proton and 16 neutrons in our model space. Therefore, particle and hole energies of protons and neutrons (ε'^π_a, ε'^ν_a) include contributions from the pp, nn, and pn particle-hole interactions to the corresponding single-particle energies (ε^π_a, ε^ν_a) in the shell-model basis such as the example expressed in Eq. (3). The relation can be written as

$$\varepsilon^i_a = \varepsilon'^i_a - \frac{1}{2j_a+1}\sum_J \sum_{b=\mathrm{hole}} (2J+1)G(ba;ba:J), \tag{4}$$

where $i = \pi$ or ν and $G(ba, ba : J)$ denotes nn and pn particle-hole interaction matrix elements since particle-hole excitations of protons are not considered in the present model space. More precisely, the symbol b in Eq. (4) refers to the two lower neutron orbits with regard to the neutron gap $N = 82$ and a denotes all the neutron and proton orbits in the present model space. The particle and hole energies observed in ^{133}Sb, ^{133}Sn, and ^{131}Sn correspond to, respectively, $\varepsilon'^\pi_{a(p)}$, $\varepsilon'^\nu_{a(p)}$, and $\varepsilon'^\nu_{a(h)}$, where the subscripts p and h mean particle and hole. Since we use the same interaction matrix elements $G(ba, ba : J)$ independent of masses for all nuclei, as mentioned above, we can determine the single-particle energies (ε^π_a, ε^ν_a) common to the nuclei through the observed particle and hole energies.

C. The parameters

We first determine the shell-model single-particle energies ε^π_a, ε^ν_a for our calculations while experiments give information only on the particle- and hole-state energies. There has been strong experimental indication from the Penning trap mass measurement that ^{132}Sn can be regarded as a quite good doubly closed-shell nucleus [39]. The magic nature of ^{132}Sn has recently been reconfirmed through an observation of single-particle states in ^{133}Sn [1]. Each of the low-lying states in ^{133}Sb is approximately a proton particle state, and that in ^{133}Sn (^{131}Sn) a neutron particle (hole) state, with respect to the magic nucleus ^{132}Sn. In the zeroth-order approximation, therefore, the proton particle energies can be taken from the experimental energies of ^{133}Sb [40] and the neutron particle (hole) energies can be taken from those of

TABLE I. The two-body force strengths (in MeV).

ii'	$g_{0,ii'}$	$g_{2,ii'}$	$\chi_{2,ii'}$	$\chi_{3,ii'}$	$\chi_{4,ii'}$
pp	0.152	0.058	0.102	0.032	0.0015
nn	0.064	0.029	0.029	0.011	0.0010
pn	0	0	0.082	0	0.0009

^{133}Sn [1] (^{131}Sn [40]). The collected single-particle energies for proton are $\varepsilon'^{\pi}_{g_{7/2}(p)} = -9.677$, $\varepsilon'^{\pi}_{d_{5/2}(p)} = -8.715$, $\varepsilon'^{\pi}_{s_{1/2}(p)} = -7.320$, $\varepsilon'^{\pi}_{d_{3/2}(p)} = -7.237$, and $\varepsilon'^{\pi}_{h_{11/2}(p)} = -6.884$ (all in MeV). The single-hole and single-particle energies for neutron are $\varepsilon'^{\nu}_{h_{11/2}(h)} = -7.377$, $\varepsilon'^{\nu}_{d_{3/2}(h)} = -7.312$, $\varepsilon'^{\nu}_{f_{7/2}(p)} = -2.470$, $\varepsilon'^{\nu}_{p_{3/2}(p)} = -1.616$, $\varepsilon'^{\nu}_{h_{9/2}(p)} = -0.909$, $\varepsilon'^{\nu}_{p_{1/2}(p)} = -1.106$, and $\varepsilon'^{\nu}_{f_{5/2}(p)} = -0.466$ (all in MeV). The only exception is $\varepsilon'^{\pi}_{s_{1/2}(p)}$, whose corresponding energy level is not experimentally known. Here we take the value suggested in Ref. [3].

We next determine the force strengths for the EPQQM Hamiltonian (1) through comparison of model calculations with the observed energy levels in the $A = 133$ nuclei ^{133}Sb and ^{133}Sn and the $A = 134$ nuclei ^{134}Te, ^{134}Sn, and ^{134}Sb. These nuclei are regarded, respectively, as the one-proton ($1p$), one-neutron ($1n$), two-proton ($2p$), two-neutron ($2n$), and one-proton-one-neutron ($1p1n$) systems beyond ^{132}Sn. Thus the procedure determines matrix elements of the pp, nn, and pn interactions, as well as the single-particle energies for the shell-model basis (3) through the relation (4) with the observed particle and hole energies. Table I summaries the determined force strengths g_0, g_2, χ_2, χ_3, and χ_4 for pp, nn, and pn interactions.

The monopole corrections used in the calculation are as follows:

$$\begin{aligned} k_{mc}^{(\nu\nu)T=1}(h_{11/2}, f_{7/2}) &= 0.04, \\ k_{mc}^{(\nu\nu)T=1}(d_{3/2}, f_{7/2}) &= 0.15, \\ k_{mc}^{(\pi\pi)T=1}(g_{7/2}, h_{11/2}) &= -0.15, \\ k_{mc}^{(\pi\nu)T=0}(g_{7/2}, h_{9/2}) &= -0.6, \\ k_{mc}^{(\pi\nu)T=0}(h_{11/2}, f_{7/2}) &= -1.0, \\ k_{mc}^{(\pi\nu)T=0}(h_{11/2}, h_{9/2}) &= -0.8. \quad \text{(in MeV)} \end{aligned} \tag{5}$$

The effects of these monopole terms will be discussed in Sec. III.

The above force strengths fix the single-particle energies $(\varepsilon_a^{\pi}, \varepsilon_a^{\nu})$ through the relation (4) with the observed particle and hole energies. $(\varepsilon_a^{\pi}, \varepsilon_a^{\nu})$ are listed in Table II, where we see that the proton single-particle energies are not modified in the present calculation.

Finally, for evaluation of electromagnetic transition probabilities, we use the standard effective charges $e_{\pi} = 1.5e$ for protons and $e_{\nu} = 0.5e$ for neutrons, and the bare g factors $g_l^{\pi} = 1$, $g_l^{\nu} = 0$, $g_s^{\pi} = 5.586$, and $g_s^{\nu} = -3.826$.

III. CALCULATED RESULTS AND DISCUSSIONS

The EPQQM Hamiltonian (1) is diagonalized in the truncated model space specified in the last section. In this section, we perform calculations for systems that have a few nucleons beyond ^{132}Sn and discuss their structure in detail. In the first and second subsections, we show that the model can basically reproduce the energy spectra in the $A = 133$ and $A = 134$ nuclei. We emphasize that both low-lying levels and high-energy states of neutron core excitations are simultaneously described. In the third subsection, we discuss the structure of the $A = 135$ nuclei ^{135}Te and ^{135}I. The success in calculation is shown through the correct reproduction of the spectra in these nuclei, among which the calculated core-excitation states in ^{135}Te are found to exhibit strong $M1$ transitions, supporting the early claim that this may be an example [41] of the classical "tilted rotation" [42] of a weakly deformed nucleus.

A. $A = 133$ nuclei ^{133}Sn and ^{133}Sb

In the following, we discuss the simplest case: the $A = 133$ nuclei with only one neutron or one proton outside the ^{132}Sn nucleus. The low-lying states of these nuclei reflect mainly the single-particle nature of neutrons or protons, and the high-energy ones test our treatment of core excitations.

1. ^{133}*Sn*

The magic character of ^{132}Sn has been demonstrated by the most recent experimental results, in the high-precision direct Penning trap mass measurement for ^{132,134}Sn [39], and the measurement of energy spectrum of ^{133}Sn [1] that has one valence neutron outside ^{132}Sn. The latter experiment [1] showed that the single-particle level $\nu p_{1/2}$ should lie below the $\nu h_{9/2}$ level, in contrast to the previous suggestion in Ref. [43]. In the present calculation, we take the neutron particle energies ε'^{ν}_a from the new experiment [1]. It should be noted that, strictly speaking, the ^{132}Sn core is not rigid, and the experimentally observed low-lying states in ^{133}Sb, ^{133}Sn, and ^{131}Sn are not pure single-particle or single-hole states but have fractions of excited states of the ^{132}Sn core. In other words, these energies are not exactly the same as $(\varepsilon'^{\pi}_a, \varepsilon'^{\nu}_a)$. We neglected the

TABLE II. The single-particle energies $(\varepsilon_a^{\pi}, \varepsilon_a^{\nu})$ (in MeV).

Proton	$0g_{7/2}$	$1d_{5/2}$	$2s_{1/2}$	$1d_{3/2}$	$0h_{11/2}$		
ε_a^{π}	−9.677	−8.715	−7.320	−7.237	−6.884		
Neutron	$0h_{11/2}$	$1d_{3/2}$	$1f_{7/2}$	$2p_{3/2}$	$0h_{9/2}$	$2p_{1/2}$	$1f_{5/2}$
ε_a^{ν}	−7.456	−7.280	−3.947	−1.945	−1.231	−1.106	−0.721

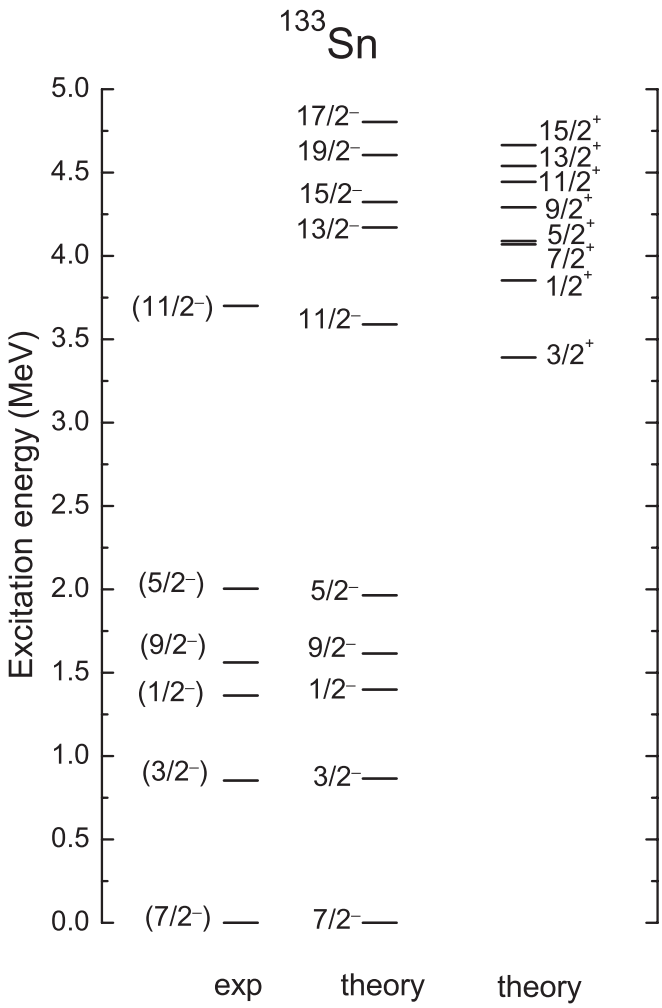

FIG. 1. Calculated energy levels of ^{133}Sn. The available experimental data, taken from Refs. [1,40], are shown for comparison.

differences by substituting the observed energies for $(\varepsilon_a'^{\pi}, \varepsilon_a'^{\nu})$ in subsection IIC (where we used the expression "zeroth-order approximation"). As shown in Fig. 1, there is a slight difference between the experimental and our calculated energy spectra of ^{133}Sn in which effects of particle-hole excitations are taken into account. Nevertheless, the difference is very small, which clearly indicates that the low-lying states (of $1/2^-$ to $9/2^-$) are almost pure single-particle states.

Going above these single-particle ones, states can be formed only at a cost of energy through core excitations. The experiment in Ref. [43] detected a $11/2^-$ state at 3.7 MeV and suggested it to be a neutron hole-excited state. As seen in Fig. 1, the present calculation correctly describes the $11/2^-_1$ state. The obtained wave function indicates that the $11/2^-_1$ state is indeed a neutron 2p-1h state with the predominant configuration $\nu(f_{7/2})^2(h_{11/2})^{-1}$, in agreement with the conclusion of Ref. [43]. Our calculation further predicts some higher-lying states from $J^\pi = 13/2^-_1$ to $19/2^-_1$ to be of the same configuration. In addition, the calculation predicts a group of core-excited states with positive parity from $J^\pi = 1/2^+_1$ to $15/2^+_1$, as shown in the right column of Fig. 1. These states, with the predominant configuration $\nu(f_{7/2})^2(d_{3/2})^{-1}$, have similar excitation energies as the predicted core-excited states of negative parity. The energies of the calculated levels depend on the monopole corrections. For example, the negative-parity states from $11/2^-$ to $17/2^-$ are modified by the monopole correction $H^{\nu\nu}_{\rm mc}(h_{11/2}, f_{7/2})$, while the predicted positive-parity states from $1/2^+$ to $15/2^+$ are dependent on the strength of $H^{\nu\nu}_{\rm mc}(d_{3/2}, f_{7/2})$. Future experiment on these states will be a strict test for our proposed interactions responsible for core excitations and the proposed monopole corrections.

In ^{133}Sn, states corresponding to the neutron $i_{13/2}$ single particle have not been seen experimentally so far. It is expected that such a state intrudes into the low-energy region as in other $N = 83$ isotones such as ^{134}Sb [8] and ^{135}Te [44]. It is our wish to include this upper-lying neutron $i_{13/2}$ orbit into our model space and, at the same time, to take neutron core excitations into account. Unfortunately, such calculations require prohibitively large amounts of computer memory when we use the NUSHELLX code. Therefore, we have not included the neutron orbit $i_{13/2}$ in the present calculations and cannot provide discussions on states that involve the neutron $i_{13/2}$ orbit.

2. ^{133}Sb

The ^{133}Sb nucleus has one valence proton outside ^{132}Sn. An experimental β-decay work was performed to study the single-proton and core-coupled states in this nucleus [45]. In Fig. 2, our shell-model results are compared with the experimental levels. The calculated energy levels for $7/2^+_1$, $5/2^+_1$, $3/2^+_1$, and $11/2^-_1$, which are proton single-particle states as confirmed by their wave functions, correspond well to the experimental ones. This indicates again, as in the ^{133}Sn case, that for these low-lying states, mixture with particle-hole excitations is very small. Our calculation suggests a $1/2^+$ state at about 2.3 MeV which has so far no experimental correspondence. This state has a predominant structure of the proton $s_{1/2}$ single particle. We note that, as in Ref. [3], our shell-model single-particle state for the proton $s_{1/2}$ orbit is an assumed value.

In Fig. 2, our model also reproduces well the high-spin states in the energy range 4 to 5 MeV for states of both positive and negative parity. The analysis of wave functions shows that these high-spin states correspond to neutron core-excited states. The positive-parity states with $J^+ \geqslant 11/2^+$ predominantly have the configuration $\pi g_{7/2}\nu f_{7/2}(h_{11/2})^{-1}$, and the negative-parity states with $J^- \geqslant 13/2^-$ mainly have the configuration $\pi g_{7/2}\nu f_{7/2}(d_{3/2})^{-1}$.

It has been reported that the nucleus ^{133}Sb has an interesting isomeric state with a half-life of 17 μs [9,10]. The recent mass measurement suggested that the isomer should have an excitation energy of 4.56 MeV with a 100-keV uncertainty nevertheless [11]. The spin and parity of the isomer are considered to be $21/2^+$, based on the shell-model calculations with the empirical nucleon-nucleon interactions [9,10]. Electromagnetic transitions directly from/to the isomeric state have not been observed, and the spin value of the isomer has not been firmly determined experimentally. At present, uncertainty in locating its excitation energy and nonobservation of the relevant transitions of the isomer make it difficult to conclude the mechanism of the isomer formation.

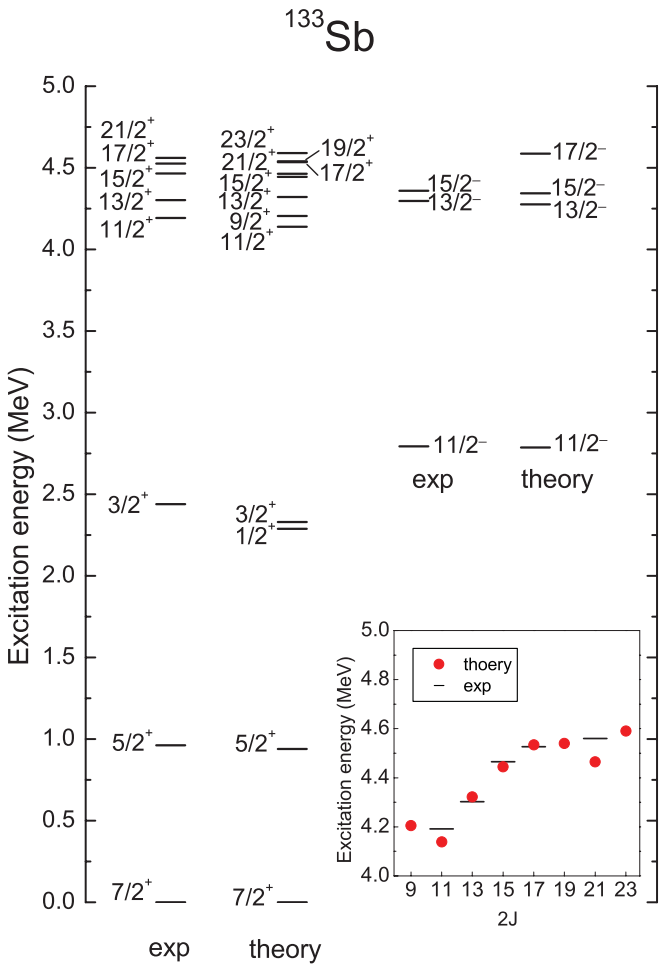

FIG. 2. (Color online) Calculated energy levels of ^{133}Sb. The available experimental data, taken from Refs. [9,11,40], are shown for comparison.

We present a detailed comparison between the calculated and experimental energy levels for the positive-parity states with $J^+ \geqslant 9/2^+$ in the inset of Fig. 2. It has been found that these states all have the same leading configuration, $\pi g_{7/2}\nu f_{7/2}(h_{11/2})^{-1}$, in agreement with the conclusions in Refs. [9,10]. Most of the known experimental levels have been precisely reproduced, with, however, one exception whereby our calculated $21/2^+$ level is notably lower than the proposed energy [11], showing clearly a reversed order with the $19/2^+$ and $17/2^+$ states. We note that the $19/2^+$ state has not been experimentally observed. With a careful parameter search, we could not easily find a set of parameters which reproduces the same order of the states (from lower to higher energy), $15/2^+_1, 17/2^+_1, 21/2^+_1$, and $19/2^+_1$, as suggested by the previous calculations [9,10]. An introduction of additional monopole terms, $H^{\nu\nu}_{\rm mc}(h_{11/2}, p_{3/2})$ and $H^{\pi\nu}_{\rm mc}(g_{7/2}, p_{3/2})$, may help pushing up the $19/2^+$ and $21/2^+$ levels from the present positions, thus producing the order of the states as proposed by Refs. [9,10]. However, the former monopole term abnormally decreases the single-particle energy ε^ν_a of the orbit $\nu 2p_{3/2}$ and the latter destroys the agreement of the $3/2^-_1$ level in ^{135}Te. Therefore, we do not prefer to adopt these monopole corrections. At present, we have to conclude that it remains a mystery to us if we are missing important correlations for a description of these states. Further experiments that can remove the above-mentioned uncertainties are very much welcome.

We now turn our discussion to some interesting consequences from the multipole interactions in the Hamiltonian (1). We first comment on the role of the hexadecupole-hexadecupole force. If we do not include the HH force in the nn interaction for ^{133}Sb, the EPQQM model lays the $17/2^+_1$ state below the $15/2^+_1$ state, which is inconsistent with the experiment. Adding the HH force to the EPQQM model changes the order of these two states, thus agreeing with the data. We find also that the HH force in the pp interaction contributes to separating the 4^+_1 and 6^+_1 states in ^{134}Te, and the HH force in the pn interaction lays the 5^-_1 state of ^{134}Sb at the right position, in accordance with results of experiment. All these results seem to indicate the effects of the HH correlations in this mass region.

The other multipole interaction that shows clear effects is the octupole-octupole type. Contrary to the experiment, the theoretical calculation obtained in Ref. [10] reversed the order of the levels $13/2^-_1$ and $15/2^-_1$. Our calculation reproduces these two states in a correct order, in which the octupole excitation for $13/2^-_1$ state discussed in Ref. [9] is confirmed. Our result shows that if the nn octupole force $\chi_{3,nn}$ is set to zero, then the $13/2^-_1$ state is almost degenerate with the $15/2^-_1$ state. In Ref. [9], a state with spin $17/2$ and unconfirmed parity was observed at 4.625 MeV. Our calculation finds a $17/2^-_1$ state at 4.587 MeV. We suggest that the experimentally observed state at 4.625 MeV could be a negative-parity, core-excited state $17/2^-_1$, which, as for the $13/2^-_1$ and $15/2^-_1$ states, belongs to the $\pi g_{7/2}\nu f_{7/2}(d_{3/2})^{-1}$ multiplet.

The nn monopole corrections $H^{\nu\nu}_{\rm mc}(h_{11/2}, f_{7/2})$ and $H^{\nu\nu}_{\rm mc}(d_{3/2}, f_{7/2})$, with the strengths listed in Eq. (5), depress the core-excited levels of both positive and negative parities, which leads to a better agreement of the theoretical energy levels with the experimental ones in ^{133}Sb. We mention that such monopole corrections are also necessary for reproducing the core-excitation states in other nuclei beyond ^{132}Sn.

B. $A = 134$ nuclei ^{134}Sn, ^{134}Te, and ^{134}Sb

The discussion in this subsection focuses on the $A = 134$ nuclei with two particles outside ^{132}Sn. These are the best examples to probe the nn, pp, and np parts of the interaction that act between the valence particles and describe core excitations.

1. ^{134}Sn

As the ^{134}Sn nucleus has two valence neutrons outside ^{132}Sn, its energy levels are sensitive to the nn part of the residual interaction. So far, only the effective interaction derived from the CD-Bonn potential [13,18] and the interactions KH5082 and CW5082 [46,47] estimated by scaling the known interactions in the ^{208}Pb region have been employed to calculate the energy levels of ^{134}Sn. In Fig. 3, we compare the obtained results from the present calculation with the known experimental levels of ^{134}Sn. Our results show that the low-energy states from 0^+_1 to 6^+_1 are almost the purely

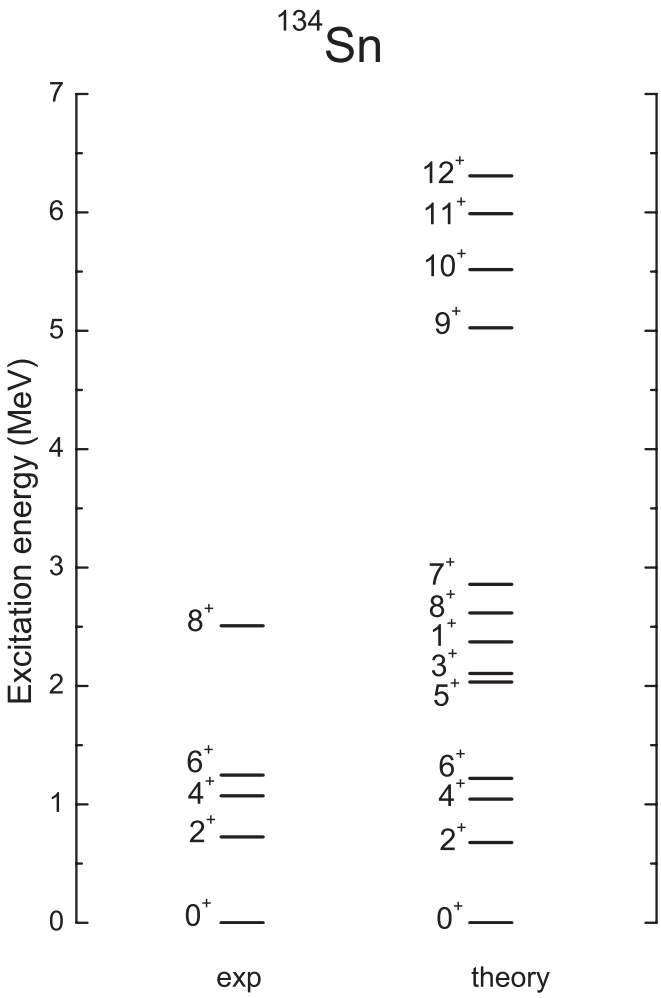

FIG. 3. Calculated energy levels of ^{134}Sn. The available experimental data, taken from Ref. [40], are shown for comparison.

correlated two-neutron states in the shells ($1f_{7/2}$, $2p_{3/2}$, $0h_{9/2}$, $2p_{1/2}$, $1f_{5/2}$), with the configuration $\nu(f_{7/2})^2$ predominating. At about 2.5 MeV the predominant configuration for the 8_1^+ state is $\nu f_{7/2}h_{9/2}$. These conclusions agree with those of the CD-Bonn calculation in Ref. [18].

In addition, our calculation predicts the yrast states 1_1^+, 3_1^+, 5_1^+, and 7_1^+ around the already-known 8_1^+ state (see Fig. 3). These states are missing in the existing experiments. The obtained wave functions indicate that the $\nu f_{7/2}h_{9/2}$ configuration predominates in the 1_1^+ and 7_1^+ states and the $\nu f_{7/2}p_{3/2}$ configuration predominates in the 3_1^+ and 5_1^+ states.

In Fig. 3, the present calculation also predicts several high-excitation states above 5 MeV with spin-parity from $J^\pi = 9^+$ to 12^+. These belong to core-excited states, which are out of the model spaces of Refs. [13,18,46]. From the obtained wave functions, we identify that the predominant configuration is $\nu(f_{7/2})^3(h_{11/2})^{-1}$ in these states. The energies of these predicted states depend on the monopole correction term $H_{\rm mc}^{\nu\nu}(h_{11/2}, f_{7/2})$, which has been adjusted to the known core-excitation level of $11/2^-$ in ^{133}Sn.

2. ^{134}Te

For ^{134}Te, the low-spin states ($J \leqslant 6$ with positive parity and $J \leqslant 9$ with negative parity) were investigated by use of the shell models using the effective interaction derived from the CD-Bonn potential [5,16,17] as well as from the KH5082 and CW5082 interactions [46,47]. These calculations, however, could not describe the core-excited states. On the other hand, the core excitation in ^{134}Te was studied in Ref. [20] with the empirical nucleon-nucleon interactions, but this study did not discuss the negative-parity states in this nucleus. The calculations performed in the present work attempt to provide a unified treatment for the entire spectrum of ^{134}Te and we investigate the structure from the low-spin states to the high-excitation ones, including both positive and negative parities.

As the ^{134}Te nucleus has two valence protons outside ^{132}Sn, the level scheme of ^{134}Te is sensitive to pp interactions. Calculated energy levels obtained for ^{134}Te are compared with the experimental data in Fig. 4. As one can clearly see, the chosen force strengths of the pp interaction and the proton

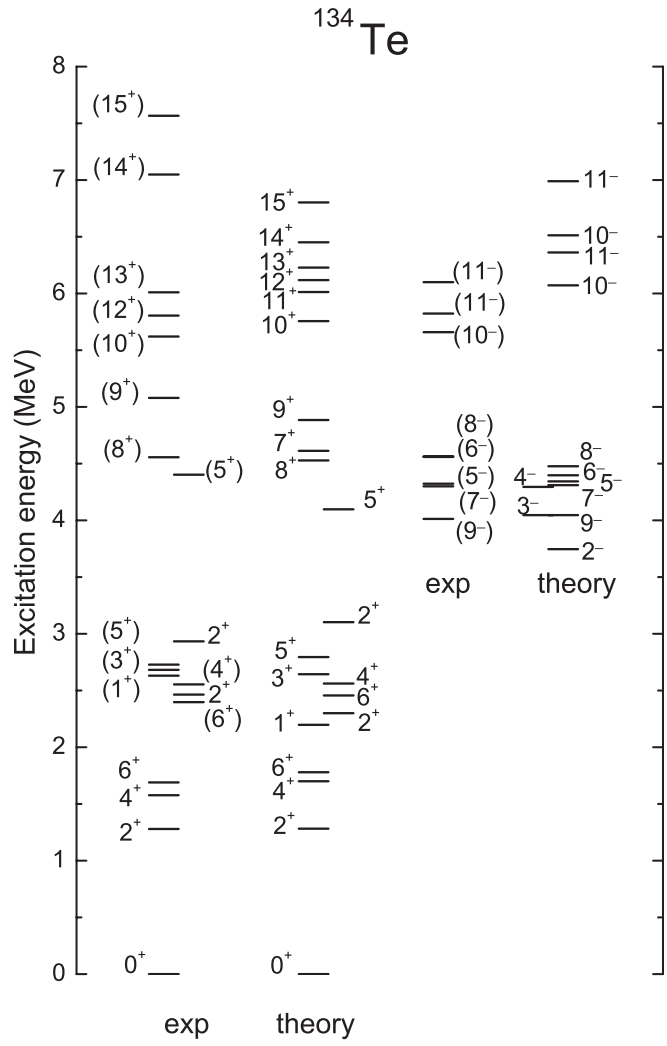

FIG. 4. Calculated energy levels of ^{134}Te. The available experimental data, taken from Refs. [36,40], are shown for comparison.

TABLE III. Comparison of calculated and experimental $B(E2)$ values for ^{134,135}Te and ^{135}I. Data are respectively taken from Refs. [7,40,46].

Nucleus	Transition	$B(E2)$ in (W.u.)	
		Expt.	Theory
^{134}Te	$2_1^+ \to 0_1^+$	6.3	4.72
	$4_1^+ \to 2_1^+$	4.3	4.92
	$6_1^+ \to 4_1^+$	2.05	2.28
	$12_1^+ \to 10_1^+$	3.2	3.50
	$11/2_1^- \to 7/2_1^-$	>0.02	5.81
^{135}Te	$15/2_1^- \to 11/2_1^-$	>6.1	6.27
	$19/2_1^- \to 15/2_1^-$	3.92	3.50
^{135}I	$15/2_1^+ \to 11/2_1^+$	2.21	4.43

single-particle energies listed in Tables I and II describe the basic feature of the experimental spectrum. The observed low-energy levels of 0_1^+, 2_1^+, 4_1^+, and 6_1^+ have been correctly reproduced. Other low-spin states observed in the energy range of 2–3 MeV are satisfactorily calculated, although the present model cannot reproduce the detailed distribution of them. The obtained wave functions suggest that these states are approximately the two-proton correlated states in the shell $(0g_{7/2}, 1d_{5/2}, 2s_{1/2}, 1d_{3/2}, 0h_{11/2})$. The states 0_1^+, 2_1^+, 4_1^+, and 6_1^+ have the predominant configuration $\pi(g_{7/2})^2$. The states 1_1^+, 3_1^+, 5_1^+ and the second exited states 2_2^+, 4_2^+, 6_2^+, which lie in the energy range of 2–3 MeV, mainly belong to the $\pi g_{7/2}d_{5/2}$ multiplet. Furthermore, our calculation reproduces the observed positive-parity 2_3^+ and 5_2^+ states at their respective energies.

Calculation of electromagnetic transition probabilities tests the shell-model wave functions. In ^{134}Te, there have been experimental measurements [7,40] of electric quadrupole transition probabilities $B(E2)$ for the even-J yrast states up to $J^\pi = 12^+$. We calculate the $B(E2)$ values by using our wave functions. The $B(E2)$ results are compared with experiment in Table III. It can be seen that the theoretical $B(E2)$ values reproduce the data quite well.

In agreement with the early works, the negative-parity states 5_1^-, 6_1^-, 7_1^-, 8_1^-, and 9_1^- in the energy range of 4–5 MeV in Fig. 4 are found to have a main configuration of $\pi g_{7/2}h_{11/2}$. We predict three more negative-parity states 2_1^-, 3_1^-, and 4_1^- belonging to the same configuration. Interestingly, we find that according to our calculation, the lowest state of the multiplet is 2^-, not 9^-. In Ref. [36], the authors showed that 9^- should be the lowest level in the $j_1 + j_2 =$ odd multiplet. We note that in the analogous example in ^{210}Po, which has two protons outside the doubly closed-shell nucleus ^{208}Pb, the level with $J_{\min} = 2$ in the $\pi h_{9/2}i_{13/2}$ multiplet lies by 174.5 keV higher than the level $J_{\max} = 11$. Applying this analogy to ^{134}Te, one would expect an higher 2_1^- state, which would require a mechanism in our model that shifts up the 2_1^- state, or the entire $j_1 + j_2 =$ even group, relative to the $j_1 + j_2 =$ odd group of the multiplet. Therefore, experimental observation of the missing 2_1^- state in ^{134}Te is very interesting.

In Ref. [36], the importance of octupole correlations in ^{134}Te was discussed. The experiment found two $E3$ transitions from the 9^- state at 4.103 MeV to two lower-lying 6^+ states. The authors suggested that there exist octupole correlations in the neighborhood of ^{132}Sn, though they are somewhat weaker than those of the ^{208}Pb region. This suggestion is reflected in our treatment because the octupole-octupole force is explicitly considered in our model. We also mention that the monopole correction $H_{\rm mc}^{\pi\pi}(g_{7/2}, h_{11/2})$ with strength of -0.15 MeV [see Eq. (5)] is responsible for placing the energies of the $\pi g_{7/2}h_{11/2}$ multiplet at the correct energy.

The positive-parity states from 8_1^+ to 15_1^+ above 4.5 MeV, and those negative-parity states 10_1^-, 11_1^-, and 11_2^- above 5.5 MeV of excitation, were suggested in Ref. [7] to be core-excited states. Our analysis of wave functions shows that the states from 8_1^+ to 15_1^+ are mainly of the configuration $\pi(g_{7/2})^2\nu f_{7/2}(h_{11/2})^{-1}$. The states 10_1^- and 11_1^- have the configuration $\pi(g_{7/2})^2\nu f_{7/2}(d_{3/2})^{-1}$, and the 11_2^- one belongs to the $\pi g_{7/2}d_{5/2}\nu f_{7/2}(d_{3/2})^{-1}$ multiplet. These results are consistent with the conclusions in Ref. [7]. The present calculations suggest two more positive-parity yrast states of core excitation, 7_1^+ and 11_1^+, which are missing in the existing experiments. We also predict a second excitation state 10_2^-, which is suggested to be a member of the $\pi(g_{7/2})^2\nu f_{7/2}(d_{3/2})^{-1}$ multiplet.

3. ^{134}Sb

Structures of the odd-odd nuclei that are adjacent to double-magic nuclei provide the best opportunities to determine the two-body proton-neutron interactions. For describing the odd-odd nucleus ^{134}Sb that has one proton and one neutron outside ^{132}Sn, the two types of effective interactions, as mentioned, have been studied extensively and applied successfully to understanding the structure of the low-spin states of this nucleus [2,18,46]. Coraggio *et al.* were able to reproduce the experimental data below 1 MeV in ^{134}Sb remarkably well [18]. In the present calculation, with the force strengths listed in Table I and the single-particle energies in Table II, we produce the energy levels up to 5.5 MeV for ^{134}Sb, as shown in Fig. 5. The experimental levels taken from Refs. [2,8,40] are drawn for comparison. As one can see, our model describes the basic feature of the experimental level scheme not only for the low-energy region but also those high excitations.

To see more details of the comparison, the low-energy 0_1^- to 7_1^- states of the theory and experiment [2] are plotted in the inset of Fig. 5. It is seen that the order of the states is correctly reproduced by the calculation. However, our calculated 1^- state lies at 151 keV in excitation and does not reproduce the observed near-degeneracy feature of it with the ground state. The early calculations found that, among various shell-model interactions, the KH208 one [2] did a good job. The calculation by Coraggio *et al.* [18] could also give the near-degeneracy feature of the 1^- state. We found that the low-excitation states up to $J^\pi = 8^-$ are approximately the correlated states of one proton from the shell $(0g_{7/2}, 1d_{5/2}, 2s_{1/2}, 1d_{3/2}, 0h_{11/2})$ and one neutron from $(1f_{7/2}, 2p_{3/2}, 0h_{9/2}, 2p_{1/2}, 1f_{5/2})$. The predominant configuration of the yrast states from 0_1^- to 7_1^- is $\pi g_{7/2}\nu f_{7/2}$, which sensitively depends on the corresponding pn interaction matrix elements. The inset of Fig. 5 indicates

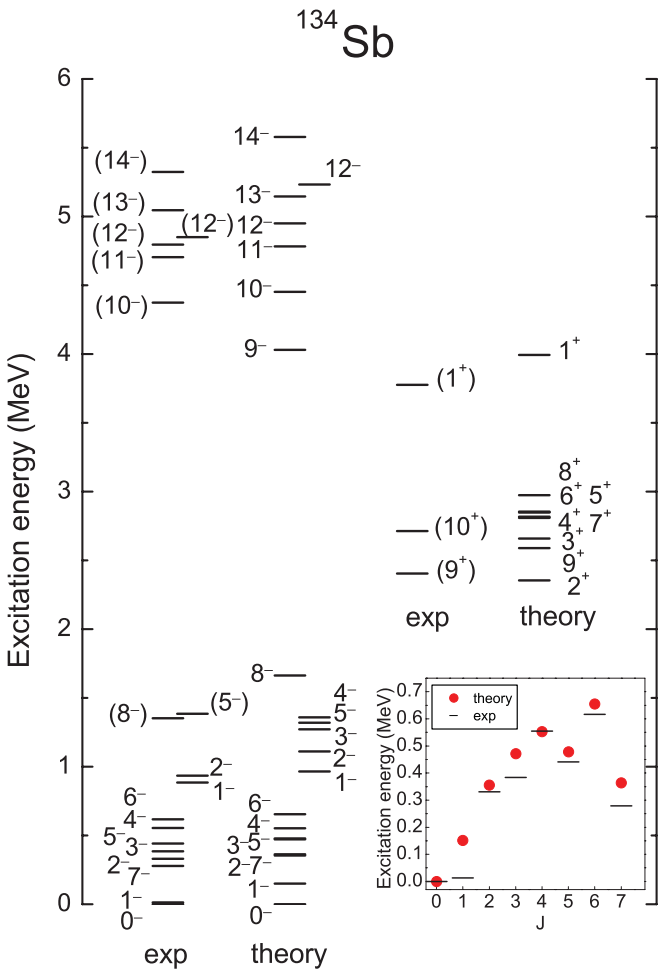

FIG. 5. (Color online) Calculated energy levels of ^{134}Sb. The available experimental data, taken from Refs. [2,40], are shown for comparison.

that our model, though showing some discrepancies, correctly traces the J-dependent variation of the states governed by the pn interactions. In other words, the EPQQM interaction can be another useful force containing the main characteristics of the pn interactions.

Near excitations of 1 MeV and above, the calculated 1_2^- state is found to have the leading configuration $\pi d_{5/2}\nu f_{7/2}$ while the 2_2^- and 5_2^- states belong to the multiplet of the configuration $(\pi g_{7/2}\nu p_{3/2})_{J=2-5}$. In Fig. 5 we predict the 3_2^- and 4_2^- states, for which the calculated wave functions show that the 4_2^- state is a member of $\pi d_{5/2}\nu f_{7/2}$ multiplet while the 3_2^- state has a mixed configuration. The higher-lying 8_1^- state has a predominant configuration of $\pi g_{7/2}\nu h_{9/2}$. We find that the monopole correction $H_{\rm mc}^{\pi\nu}(g_{7/2}, h_{9/2})$ given in Eq. (5) plays a role to lower the 8_1^- state to the observed energy, but the pn components in the $J = 0$ and $J = 2$ pairing forces and in the octupole-octupole force can be neglected (see Table I).

For the negative-parity states, there is a 2-MeV gap between the low-energy region and high-spin states. Obviously, the high-spin states with $J^\pi \geqslant 9^-$ cannot be generated without core excitation of neutrons. The present calculation reproduces well the observed states from 10_1^- to 14_1^-. In addition, we predict a 9_1^- state below the 10_1^- state. Consistent with the discussion in Ref. [8], our calculated wave functions indicate that the main configuration of these states is $\pi g_{7/2}\nu(f_{7/2})^2(h_{11/2})^{-1}$. The experiment in Ref. [8] detected the 12_2^- state with the excitation energy 4.57 MeV relative to the 7_1^- state. This state was considered to have the main configuration $\pi h_{11/2}\nu i_{13/2}$, which is out of our model space without considering the $\nu i_{13/2}$ orbit. In Fig. 5, we find a 12_2^- state from the calculation, which, however, belongs to the neutron core-excited configuration $\pi g_{7/2}\nu(f_{7/2})^2(h_{11/2})^{-1}$.

There have been a few observed positive-parity states (9^+, 10^+, and 1^+) in ^{134}Sb. According to Ref. [8], the 10^+ state was considered to be of the configuration $\pi g_{7/2}\nu i_{13/2}$. This configuration is, again, out of our model space. As shown in Fig. 5, the other two observed 9^+ and 1^+ states are well reproduced by our model. The calculated states of 9^+ and 1^+ have the leading configurations of $\pi h_{11/2}\nu f_{7/2}$ and $\pi h_{11/2}\nu h_{9/2}$, respectively. Their correct description is obtained with the help of the monopole correction $H_{\rm mc}^{\pi\nu}(h_{11/2}, f_{7/2})$ with the strength -1.0 MeV and $H_{\rm mc}^{\pi\nu}(h_{11/2}, h_{9/2})$ with the strength -0.8 MeV [see Eq. (5)]. These two monopole terms depress the energy levels 9^+ and 1^+ to the right energies but do not affect the negative-parity energy levels. The present model predicts an existence of other members of the $\pi h_{11/2}\nu f_{7/2}$ multiplet with $J^\pi = 2^+$ to 8^+ around the 9^+ level (see Fig. 5).

C. $A = 135$ nuclei ^{135}Te and ^{135}I

The EPQQM model parameters have been determined by studying the $A = 133$ and $A = 134$ nuclei, as discussed above. The model can be tested by calculations for the $A = 135$ nuclei which have three particles outside ^{132}Sn. In this subsection, we discuss two $A = 135$ nuclei, namely ^{135}Te and ^{135}I. Calculations for the rest of $A = 135$ nuclei require a prohibitively large amount of computer memory if we consider core excitations, and, therefore, we leave those calculations for future works.

1. ^{135}Te

The nucleus ^{135}Te was previously studied in Refs. [5,46], where the low-energy negative-parity states below the state $21/2^-$ were calculated. In the present work, we study all the observed negative-parity states up to the high-spin state $J^\pi = 35/2^-$ and some positive-parity states. The calculated energy levels are compared with experimental ones in Fig. 6. The figure shows that our model, with the parameters determined for lighter nuclei, describes ^{135}Te quite well.

The low-lying states below 3 MeV, as those studied in Refs. [5,46], can be created without neutron core excitations. The early analysis in Ref. [48] regarded the states from $1/2_1^-$ to $9/2_1^-$ simply as the neutron single-particle states coupled to the $J = 0$ proton pair in the $g_{7/2}$ orbit, $\pi(g_{7/2})^2_{J=0}$. The present calculation confirms this simple picture, except for the $5/2_1^-$ state. We have found that the yrast states $1/2_1^-$, $3/2_1^-$, $7/2_1^-$, and $9/2_1^-$ consist approximately of a neutron in the single-particle orbit and a proton pair with $J = 0$ distributed to the proton orbits ($0g_{7/2}$, $1d_{5/2}$, $2s_{1/2}$, $1d_{3/2}$, $0h_{11/2}$). The

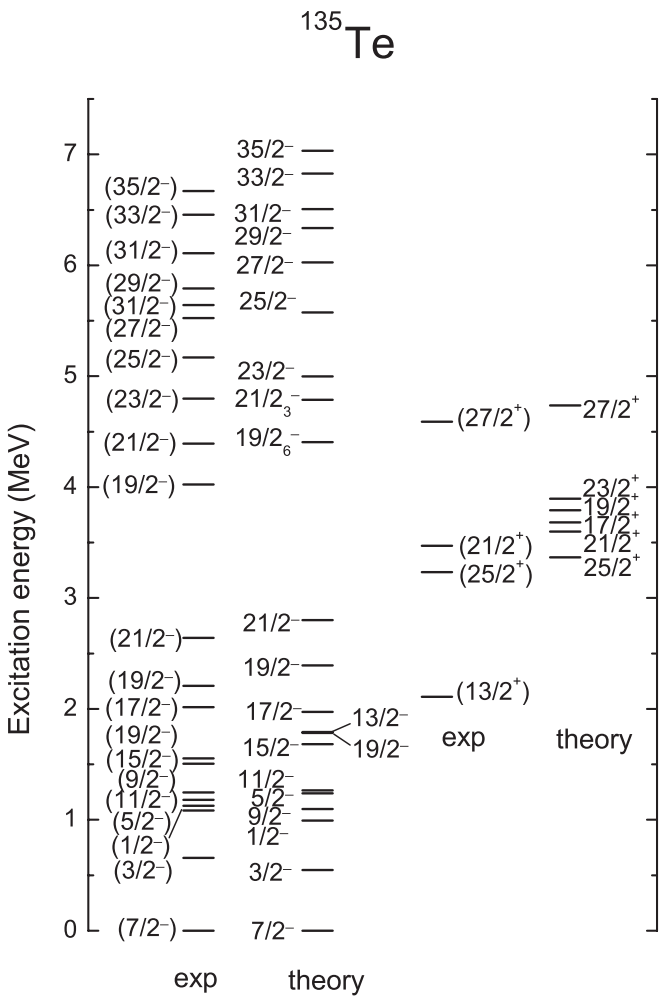

FIG. 6. Calculated energy levels of ^{135}Te. The available experimental data, taken from Ref. [40], are shown for comparison.

$5/2^-_1$ state, however, has been found to have a predominant configuration of $\pi(g_{7/2})^2_{J>0}\nu f_{7/2}$, in which the two protons contribute nonzero angular momenta and the neutron is in the $f_{7/2}$ orbit. The yrast states from $11/2^-_1$ to $19/2^-_1$ are found also to be of this configuration. The $21/2^-_1$ state has a predominant configuration $\pi(g_{7/2})^2\nu h_{9/2}$. Its excitation energy is depressed by the monopole correction $H^{\pi\nu}_{\rm mc}(g_{7/2}, h_{9/2})$ adopted in Eq. (5). We finally note that the $19/2^-_2$ state has the main configuration $\pi g_{7/2}d_{5/2}\nu f_{7/2}$.

It is known that the $19/2^-_1$ state is an isomeric state with lifetime 0.5 μs [8]. Our model reproduces the $19/2^-_1$ isomeric state at a correct position along with the other states of the same multiplet. Our calculation also gives correctly the $B(E2)$ values for the cascade decays from the isomeric state, as shown in Table III. The isomeric nature of the $19/2^-_1$ state is attributed to the fact that the $17/2^-_1$ state lies above the isomeric state and the $E2$ decay from the $19/2^-_1$ state to $15/2^-_1$ is hindered because of a small energy separation between these two states.

The negative-parity high-spin states above 4 MeV are created by participation of neutron core excitations. The calculation using the empirical nucleon-nucleon interaction in Ref. [8] could not describe these states. In Fig. 6, our calculation demonstrates that the EPQQM interaction reproduces successfully these high-spin states with inclusion of neutron core excitations. We have found that all these states have a predominant configuration $\pi(g_{7/2})^2\nu(f_{7/2})^2(h_{11/2})^{-1}$, with an exception of the $25/2^-_1$ state, which has the leading configuration $\pi(g_{7/2})^2\nu f_{7/2}h_{9/2}(h_{11/2})^{-1}$. However, our model cannot give the $31/2^-_1$ state at 5.641 MeV observed in Ref. [8]. That state has possibly the configuration $\pi g_{7/2}h_{11/2}\nu i_{13/2}$, which is out of the present model space.

In Ref. [41], the observed strong $J \to J-1$ cascade transitions (presumably $M1$ according to the authors) and weak crossover $J \to J-2$ transitions within the high-spin negative parity states in ^{135}Te were explored. The authors suggested [41] that this is possibly an example of "tilted rotation" of a weakly deformed nucleus [42], which is caused in this case by a participation of a neutron hole in the $h_{11/2}$ orbit. Large ratios of $B(M1; J \to J-1)/B(E2; J \to J-2)$ for decays from respective J states can be the most important fingerprint to define the so-called magnetic rotation band [49]. Using our wave functions, we have calculated the $B(M1)$ values for the cascade transitions and the $B(E2)$ values for the crossover $E2$ transitions for the states from $19/2^-$ to $35/2^-$. The calculated transition probabilities are illustrated in Fig. 7. The band structure seems to be disturbed a bit by the predicted different configuration of the $25/2^-$ state, as discussed above. Nevertheless, overwhelmingly large $M1$ transitions over $E2$ are clearly seen from our calculations. The average $B(M1; J \to J-1)/B(E2; J \to J-2)$ ratio for the cascade is about 17 $(\mu_N/eb)^2$, with the smallest ratio, $\approx$3.2 $(\mu_N/eb)^2$, for the transition from the $J^\pi = 23/2^-_1$ state. This implies that such core-excitation states indeed generate a quite large magnetic dipole moment and exhibit the main feature of a magnetic rotation band.

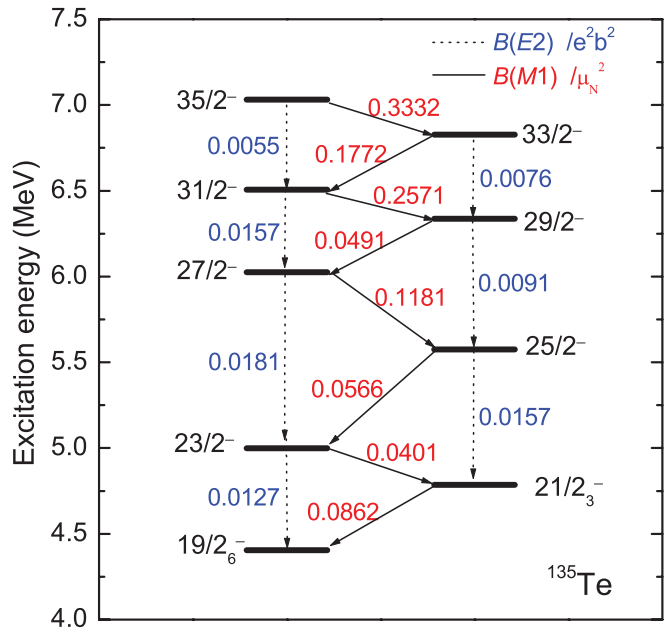

FIG. 7. (Color online) Calculated $B(E2)$ and $B(M1)$ values for the core-excitation states in ^{135}Te.

The experimentally detected [8] positive-parity states $25/2^+$, $21/2^+$, and $27/2^+$ are compared with calculated energy levels in the right column of Fig. 6. The present calculation nicely reproduces these levels and predicts additional states $17/2^+$, $19/2^+$, and $23/2^+$ above the $21/2^+$ state, as shown in Fig. 6. From the calculation, the states $17/2_1^+$ to $25/2_1^+$ have the leading configuration $\pi g_{7/2}h_{11/2}\nu f_{7/2}$, but the state $27/2_1^+$ demands another configuration $\pi g_{7/2}h_{11/2}\nu h_{9/2}$ to attain its high spin $J = 27/2$. We have found that the monopole corrections $H_{\rm mc}^{\pi\pi}(g_{7/2}, h_{11/2})$ and $H_{\rm mc}^{\pi\nu}(h_{11/2}, f_{7/2})$, determined for lighter nuclei, are effective for laying the $21/2^+$ and $25/2^+$ states at respective positions, and $H_{\rm mc}^{\pi\pi}(g_{7/2}, h_{11/2})$ and $H_{\rm mc}^{\pi\nu}(h_{11/2}, h_{9/2})$ have corporative effects on the $27/2^+$ state. The experiment [44] detected another state $13/2^+$ at 2.109 MeV as the neutron single-particle state $i_{13/2}$, which is out of our model space and cannot be produced in the present calculations.

2. ^{135}I

Last, we discuss the structure of the nucleus ^{135}I which has three protons outside ^{132}Sn. The previous works [5,17,46] calculated the low-excitation levels below 4 MeV in this nucleus, and the work with the empirical nucleon-nucleon interaction [20] calculated those positive-parity states of particle-hole excitations. In the present calculation, we consistently deal with all these states, which produces the positive-parity states up to $27/2^+$ and the negative-parity states up to $25/2^-$ (roughly 6 MeV in excitation). Figure 8 shows the calculated energy levels compared with the available experimental data. As one can see, all the known energy levels in ^{135}I are well described. Our EPQQM interaction reproduces the known low-lying positive-parity levels with $J^\pi \leqslant 17/2^+$ and the negative-parity levels $19/2^-$, $23/2^-$, and $21/2^-$ at the respective energies and in a correct order.

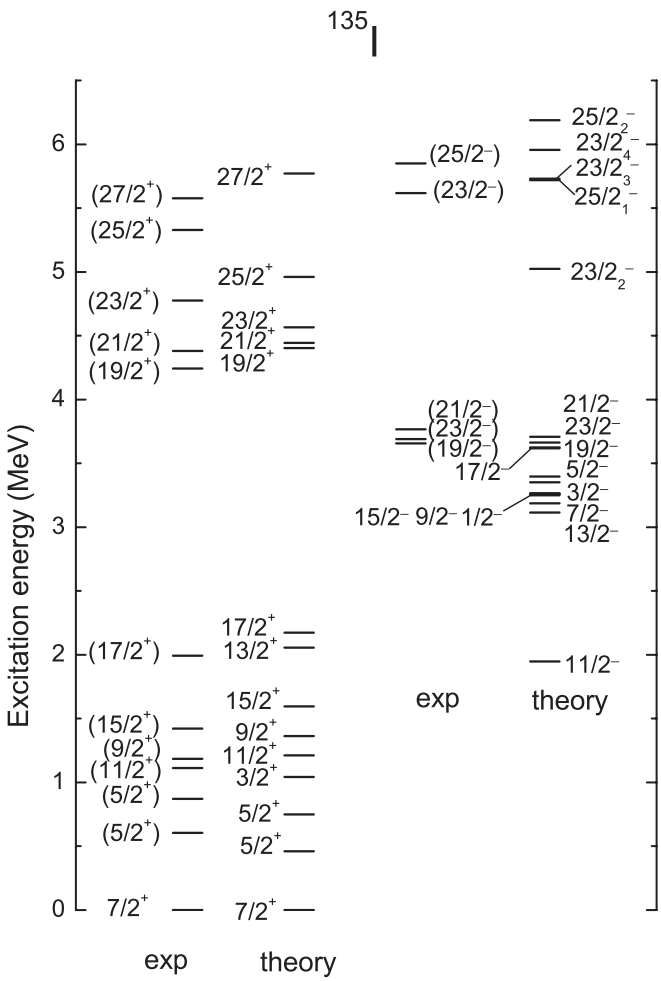

FIG. 8. Calculated energy levels of ^{135}I. The available experimental data, taken from Ref. [40], are shown for comparison.

The lowest-energy configuration $\pi(g_{7/2})^3$ can create the states with spins $3/2^+$, $5/2^+$, $7/2^+$, $9/2^+$, $11/2^+$, and $15/2^+$. Our calculated wave functions indicate undoubtedly that the states $3/2_1^+$, $7/2_1^+$, $9/2_1^+$, $11/2_1^+$, and $15/2_1^+$ have the predominant configuration $\pi(g_{7/2})^3$. Interestingly, the predominant configuration of the lower $5/2_1^+$ state is $\pi(g_{7/2})^2 d_{5/2}$ while the $5/2_2^+$ state has the main configuration $\pi(g_{7/2})^3$. The states $13/2_1^+$ and $17/2_1^+$ are found to be the members of the same multiplet as $5/2_1^+$.

Separated by a 2-MeV energy gap from the low-lying states, the positive-parity states from $19/2_1^+$ to $27/2_1^+$ above 4 MeV are neutron core-excited states, having the predominant configuration $\pi(g_{7/2})^3\nu f_{7/2}(h_{11/2})^{-1}$. Our EPQQM interaction reproduces the energy levels of these high-energy states at fairly good energies and in a correct order.

The negative-parity states $19/2_1^-$, $23/2_1^-$, and $21/2_1^-$ between 3 and 4 MeV are created by one proton excited from the low orbit $g_{7/2}$ into the high-j orbit $h_{11/2}$. The predominant configuration is $\pi(g_{7/2})^2 h_{11/2}$. The calculated states $1/2_1^-$ to $17/2_1^-$ are suggested also to be members of this multiplet with the main configuration $(\pi(g_{7/2})^2 h_{11/2})_{J=1/2-23/2}$. We point out that the monopole correction $H_{\rm mc}^{\pi\pi}(g_{7/2}, h_{11/2})$, determined earlier, contributes to placing the states $19/2_1^-$ to $23/2_1^-$ at respective energies. This is the same effect as mentioned for ^{134}Te in the previous subsection.

The two negative-parity levels $23/2^-$ and $25/2^-$ observed above 5.5 MeV belong to core-excitation states. They were identified as the members of the $\pi(g_{7/2})^3\nu f_{7/2}(d_{3/2})^{-1}$ multiplet in Ref. [7]. In our calculation, the $23/2_4^-$ state and the $25/2_2^-$ state have the predominant configuration $\pi(g_{7/2})^3\nu f_{7/2}(d_{3/2})^{-1}$. The present model gives almost degenerate states $23/2_3^-$ and $25/2_1^-$ below the $23/2_4^-$ state. They are also core-excitation states and both are members of the $\pi(g_{7/2})^2 h_{11/2}\nu f_{7/2}(d_{3/2})^{-1}$ multiplet. So their positions for the energy level are lowered greatly by the monopole correction $H_{\rm mc}^{\pi\nu}(h_{11/2}, f_{7/2})$ with strength of -1.0 MeV in Eq. (5).

Our model also predicts the $23/2_2^-$ state, having the predominant configuration $\pi g_{7/2}d_{5/2}h_{11/2}$. The above results confirm the previous analysis in Ref. [7]. Moreover, the present calculation provides new information for the $5/2^+$, $23/2^-$, and $25/2^-$ states, and so on. We calculated the $B(E2)$ value for the transition $15/2_1^+ \to 11/2_1^+$ and compared it with the experiment cited in Ref. [46]. The comparison is shown in Table III. The theoretical value of $B(E2; 15/2_1^+ \to 11/2_1^+)$ is twice that of the experiment. We hope that more experimental $B(E2)$ values for other states will come out in the future to test our model predictions.

IV. CONCLUSIONS

The study of neutron-rich nuclei beyond the doubly magic nucleus ^{132}Sn has been at the forefront of current nuclear structure research. One of the most challenging problems in shell-model calculations is to find suitable effective interactions that work for the description of both low-lying states and core excitations. The theoretical development reported in this article represents an attempt toward this goal and is very relevant for the ongoing experimental program of CARIBU at Argonne National Laboratory.

By means of large-scale shell-model calculations, we have carried out a systematic study of the $A = 133$–135 nuclei that have a few nucleons outside ^{132}Sn. The calculation includes neutron core excitations across the $N = 82$ shell gap. The employment of the EPQQM model has made it possible to define the effective pp, nn, and pn interactions for a considerably large model space, which consists of the proton shells $0g_{7/2}$, $1d_{5/2}$, $2s_{1/2}$, $1d_{3/2}$, and $0h_{11/2}$ and neutron shells $0h_{11/2}$, $1d_{3/2}$, $1f_{7/2}$, $2p_{3/2}$, $0h_{9/2}$, $2p_{1/2}$, and $1f_{5/2}$. With a set of well-determined parameters, the model has explained the experimental energy levels, not only the low-energy states but also those high-energy ones in ^{133}Sn, ^{133}Sb, ^{134}Sn, ^{134}Te, ^{134}Sb, ^{135}Te, and ^{135}I. The fairly good agreement of the calculated $B(E2)$ values with the available experimental data indicates that the basic structure of these nuclei can be well described by the present model. This paper, together with the previous publications in Refs. [24–26], has demonstrated the ability of the EPQQM model for explaining various nuclei in which protons and neutrons occupy different shells. The effective interaction with the separable forces derived from the EPQQM model has been proven to be capable of capturing the main physics of core excitations in the ^{132}Sn mass region. As a representative example, we have investigated the ratios of $B(M1)/B(E2)$ for the particle-hole excitation states in ^{135}Te to examine the suggestion of Ref. [41] about a possible magnetic rotation band. The present shell-model calculation has shown that the core-excitation states in this nucleus have indeed quite a large magnetic moment, thus supporting the picture of the so-called magnetic rotation.

The present calculations have also confirmed the importance of octupole correlations in this mass region and, furthermore, suggested the existence of hexadecupole correlations. The good results have been obtained with the help of several monopole corrections in the model that have been adjusted to existing experimental data. Many predictions, in particular those predicting high-energy states formed by core excitations, await future experimental confirmation, which would test rigorously our proposed interactions.

ACKNOWLEDGMENTS

One of us (M. H.) thanks colleagues of Department of Physics for the hospitality extended to him when he visited Shanghai Jiao Tong University (SJTU), and he is grateful for support from the SJTU-INS Research Project for Visiting Scholars. Research at SJTU was supported by the National Natural Science Foundation of China under Contract No. 11075103, the Shanghai Pu-Jiang grant, and the Chinese Academy of Sciences.

[1] K. L. Jones *et al.*, Nature **465**, 454 (2010).
[2] J. Shergur *et al.*, Phys. Rev. C **71**, 064321 (2005).
[3] J. Shergur *et al.*, Phys. Rev. C **72**, 024305 (2005).
[4] C. Goodin *et al.*, Phys. Rev. C **78**, 044331 (2008).
[5] S. H. Liu *et al.*, Phys. Rev. C **81**, 014316 (2010).
[6] A. Korgul *et al.*, Eur. Phys. J. A **15**, 181 (2002).
[7] S. K. Saha *et al.*, Phys. Rev. C **65**, 017302 (2001).
[8] B. Fornal *et al.*, Phys. Rev. C **63**, 024322 (2001).
[9] W. Urban *et al.*, Phys. Rev. C **62**, 027301 (2000); W. Urban, A. Złomaniec, G. S. Simpson, H. Faust, T. Rząca-Urban, and M. Jentschel, *ibid.* **79**, 037304 (2009).
[10] J. Genevey, J. A. Pinston, H. Faust, C. Foin, S. Oberstedt, and B. Weiss, Eur. Phys. J. A **7**, 463 (2000).
[11] B. Sun *et al.*, Phys. Lett. B **688**, 294 (2010).
[12] S. Sarkar and M. Saha Sarkar, Phys. Rev. C **81**, 064328 (2010).
[13] M. P. Kartamyshev, T. Engeland, M. Hjorth-Jensen, and E. Osnes, Phys. Rev. C **76**, 024313 (2007).
[14] H. Grawe, K. Langanke, and G. Martínez-Pinedo, Rep. Prog. Phys. **70**, 1525 (2007).
[15] G. Martínez-Pinedo and K. Langanke, Phys. Rev. Lett. **83**, 4502 (1999).
[16] F. Andreozzi, L. Coraggio, A. Covello, A. Gargano, T. T. S. Kuo, and A. Porrino, Phys. Rev. C **56**, R16 (1997).
[17] L. Coraggio, A. Covello, A. Gargano, N. Itaco, and T. T. S. Kuo, Phys. Rev. C **80**, 044320 (2009).
[18] L. Coraggio, A. Covello, A. Gargano, and N. Itaco, Phys. Rev. C **65**, 051306(R) (2002); **72**, 057302 (2005); **73**, 031302(R) (2006).
[19] B. A. Brown, N. J. Stone, J. R. Stone, I. S. Towner, and M. Hjorth-Jensen, Phys. Rev. C **71**, 044317 (2005).
[20] C. T. Zhang *et al.*, Phys. Rev. Lett. **77**, 3743 (1996).
[21] M. Hasegawa and K. Kaneko, Phys. Rev. C **59**, 1449 (1999).
[22] M. Hasegawa, K. Kaneko, and S. Tazaki, Nucl. Phys. A **674**, 411 (2000); **688**, 765 (2001).
[23] K. Kaneko, Y. Sun, M. Hasegawa, and T. Mizusaki, Phys. Rev. C **78**, 064312 (2008).
[24] Y. H. Zhang *et al.*, Phys. Rev. C **79**, 044316 (2009).
[25] M. Hasegawa, Y. Sun, S. Tazaki, K. Kaneko, and T. Mizusaki, Phys. Lett. B **696**, 197 (2011).
[26] K. Kaneko, Y. Sun, T. Mizusaki, and M. Hasegawa, Phys. Rev. C **83**, 014320 (2011).
[27] L. S. Kisslinger and R. A. Sorensen, Rev. Mod. Phys. **35**, 853 (1963).
[28] M. Baranger and K. Kumar, Nucl. Phys. A **110**, 490 (1968); **110**, 529 (1968); **122**, 241 (1968).
[29] T. Kishimoto and T. Tamura, Nucl. Phys. A **192**, 246 (1972); **270**, 317 (1976).
[30] K. Hara and Y. Sun, Int. J. Mod. Phys. E **4**, 637 (1995).
[31] M. Dufour and A. P. Zuker, Phys. Rev. C **54**, 1641 (1996).
[32] J. Duflo and A. P. Zuker, Phys. Rev. C **59**, R2347 (1999).

[33] M. Górska *et al*., Phys. Lett. B **672**, 313 (2009).
[34] T. Otsuka, T. Suzuki, R. Fujimoto, H. Grawe, and Y. Akaishi, Phys. Rev. Lett. **95**, 232502 (2005).
[35] T. Otsuka, T. Suzuki, M. Honma, Y. Utsuno, N. Tsunoda, K. Tsukiyama, and M. Hjorth-Jensen, Phys. Rev. Lett. **104**, 012501 (2010).
[36] J. P. Omtvedt, H. Mach, B. Fogelberg, D. Jerrestam, M. Hellström, L. Spanier, K. I. Erokhina, and V. I. Isakov, Phys. Rev. Lett. **75**, 3090 (1995).
[37] B. Fogelberg, M. Hellström, D. Jerrestam, H. Mach, J. Blomqvist, A. Kerek, L. O. Norlin, and J. P. Omtvedt, Phys. Rev. Lett. **73**, 2413 (1994).
[38] W. Rae, the paper and the NUSHELLX code [http://knollhouse.org.].
[39] M. Dworschak *et al*., Phys. Rev. Lett. **100**, 072501 (2008).
[40] [http://www.nndc.bnl.gov/ensdf/].
[41] Y. X. Luo *et al*., Phys. Rev. C **64**, 054306 (2001).
[42] S. Frauendorf, Nucl. Phys. A **557**, 259c (1993).
[43] P. Hoff *et al*. (ISOLDE Collaboration), Phys. Rev. Lett. **77**, 1020 (1996).
[44] C. J. Gross, J. Phys. G **31**, S1639 (2005).
[45] M. Sanchez-Vega, B. Fogelberg, H. Mach, R. B. E. Taylor, A. Lindroth, J. Blomqvist, A. Covello, and A. Gargano, Phys. Rev. C **60**, 024303 (1999).
[46] S. Sarkar and M. S. Sarkar, Phys. Rev. C **64**, 014312 (2001).
[47] W.-T. Chou and E. K. Warburton, Phys. Rev. C **45**, 1720 (1992).
[48] P. Hoff, B. Ekström, and B. Fogelberg, Z. Phys. A **332**, 407 (1989).
[49] H. Schnare *et al*., Phys. Rev. Lett. **82**, 4408 (1999).